ENTHALPY MEASUREMENTS ON LiNO$_3$ AND NaNO$_2$ BY TWIN HIGH-TEMPERATURE CALORIMETER

MASAYUKI KAMIMOTO

Energy Division, Electrotechnical Laboratory, Sakura-mura, Niihari-gun, Ibaraki (Japan)

(Received 29 April 1980)

ABSTRACT

A high-temperature calorimeter of the twin type designed for the enthalpy measurement of latent-heat storage materials is described. The measured enthalpy change of the N.B.S. calorimetric standard sapphire was in agreement with N.B.S. data within ±1.5% from room temperature up to 400°C. The enthalpy changes of LiNO$_3$ and NaNO$_2$ were determined through the fusion up to 300°C. Their enthalpies of fusion and heat capacities are presented.

INTRODUCTION

The importance of thermal energy storage has been increasing in the field of energy technology [1]. Thermodynamic properties are among the most important information for screening good thermal energy storage materials [2] and also for designing storage systems. Reliable data, however, do not always exist even for simple compounds. The enthalpy of LiNO$_3$ has already been measured by Goodwin and Kalmus [3], though the reliability of their data, as they point out, is not high because of the hygroscopic nature of LiNO$_3$. Cases [4] investigated NaNO$_2$ by drop calorimetry and pointed out that the heat capacity of the liquid is much lower than that of the solid. Direct heat capacity measurements have been done only in a limited temperature range near the λ transition of NaNO$_2$ [5—7]. Since LiNO$_3$ and NaNO$_2$ are considered to be possible latent-heat storage materials and/or the component materials at medium temperatures [8], it is necessary to determine the enthalpy of these salts through the fusion. The purpose of this study is to construct a calorimeter with an operating temperature range from 300 to 1000 K and to measure the enthalpy changes of LiNO$_3$ and NaNO$_2$.

A high-temperature calorimeter of the twin type was first designed by Kleppa [9] to measure the enthalpy of mixing of liquid melts, such as molten salts, and was proved to be a good choice for this kind of measurement at high temperatures. Recently, it has also been used to measure the temperature dependence of the enthalpy (enthalpy change) of a few materials including PbF$_2$ [10] and BeF$_2$ [11] through the diffuse transition and the melting points, respectively, and has proved to be reasonably reliable for the enthalpy change measurement.

Because its reliability and comparatively low cost of construction, we have made a calorimeter of this type. It can be used to measure the enthalpy of reactions appropriate to chemical storage as well as the enthalpy change of latent-heat storage materials.

In the present study, the calorimeter constructed has been calibrated and tested with joule heating and the NBS calorimetric standard sapphire. The enthalpy changes of $LiNO_3$ and $NaNO_2$ have been then measured over the temperature range through the fusion.

EXPERIMENTAL

Apparatus and method of measurement

The calorimeter is shown in Fig. 1. Although it is almost the same as the apparatus of other investigators, it differs from them in the materials used. In addition to this, more thermocouples have been used in order to increase the sensitivity, even with platinum/platinum—rhodium thermocouples, and also to realize good proportionality between the enthalpy change in the calorimeter cell and the integral of the differential temperature.

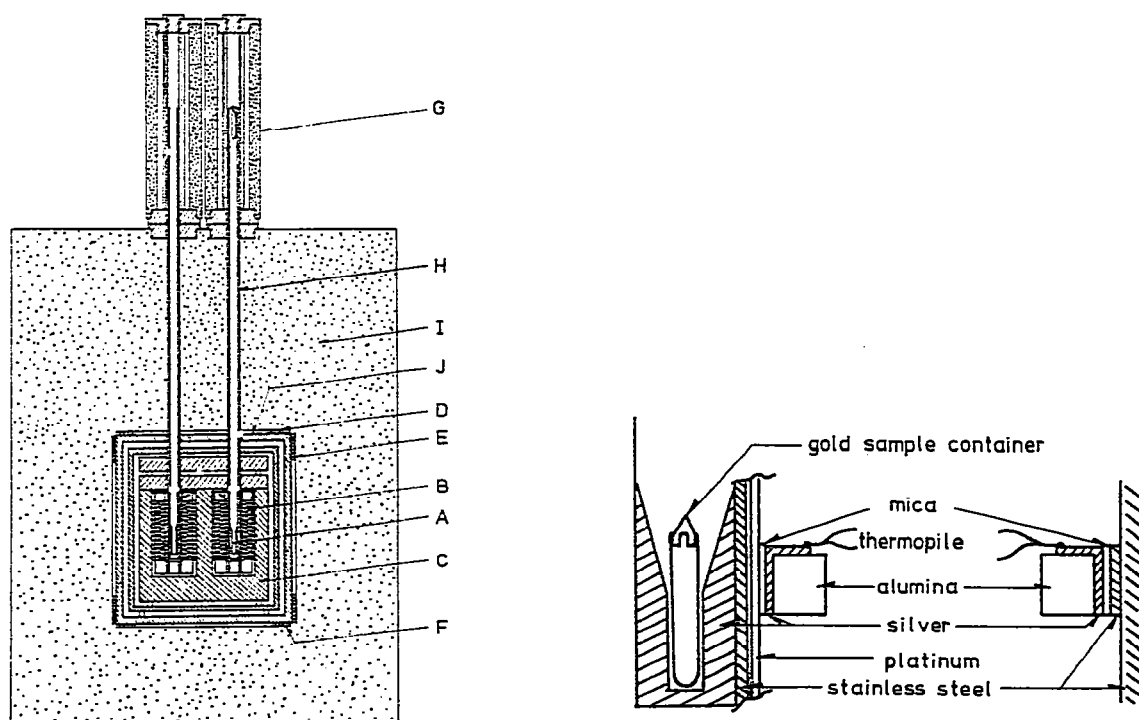The calorimeter consists of two nearly identical differential calorimetric

Fig. 1. Layout of twin high-temperature calorimeter. A, Calorimeter cell; B, thermopile; C, stainless steel jacket; D, top heater; E, main heater; F, bottom heater; G, upper furnace; H, protection tube; I, quartz wool; J, heavy shield.

Fig. 2. Detail of calorimetric unit.

units located in two cylindrical wells in a jacket made of stainless steel. Details of part of the calorimetric unit are presented in Fig. 2. The temperature difference between the unit and the jacket is detected by a thermopile for each unit, which is composed of 128 platinum/platinum—rhodium thermocouples connected as follows. Eight thermocouples are connected in a checkerboard pattern on the surface of thin silver plates, which are insulated by mica from the jacket and from the platinum foil cover around the stainless steel protection tube. The thermocouples, silver plates, and mica are supported by alumina rings sintered to fit the jacket and the tube as shown in Fig. 2. Sixteen such assemblies are arranged in the same manner. The two thermopiles are connected in series, and in opposition to each other. Each calorimeter cell consists of the stainless steel protection tube and the silver block.

The temperature of the jacket was kept constant by three heaters separately wound around the heavy carbon steel shield and controlled by independent SCR controllers. The temperature of the calorimeter cell was measured with a calibrated chromel—alumel thermocouple placed in the opposite calorimeter cell to that used for the specimen. Calibration of the thermocouple was carried out at the melting points of aluminium, zinc, tin, and lead. During operation, dried nitrogen gas was passed through the calorimeter to protect the materials from oxidation.

When the temperature dependence of the enthalpy was measured, two small furnaces were placed on the calorimeter to maintain the specimen at the desired temperature before a drop and also to keep the conditions of the two calorimetric units almost identical. To obtain a constant temperature profile in such small furnaces at high temperatures, a silver cylinder was placed in each furnace and a specimen was set inside the cylinder as shown in Fig. 3. When a constant temperature profile of less than ±0.2 K inside the cylinder was confirmed, the temperature of the specimen before a drop was measured by a chromel—alumel thermocouple located inside the cylinder. This thermocouple was calibrated by a comparison method against the calibrated thermocouple used for measuring the temperature of the calorimeter cell.

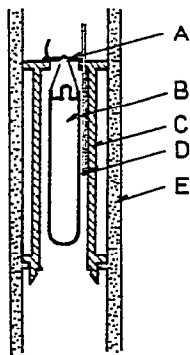The signal of the differential temperature detected by the thermopiles was

Fig. 3. Detail of sample holding device in the upper furnace. A, Alumina rod; B, sample container; C, silver cylinder; D, chromel—alumel thermocouple; E, stainless steel tube.

TABLE 1

Masses of specimens and containers

Specimen	Mass (g)	
	Specimen	Container
Sapphire	2.1870	5.0621
LiNO$_3$	2.1116	5.3494
NaNO$_2$	1.6824	5.3137

preamplified by a Model CAM-1001 amplifier (Tokyo Riko Co.) and then fed to a Model CI-3 integrator (Tokyo Riko Co.). Both the differential temperature and its time integral were recorded with a Model 3056-22 two-pen recorder (Yokogawa Electric Works Ltd.).

Samples

The sapphire sample used for the calibration and test of the calorimeter was the N.B.S. calorimetric standard No. 720. The samples of LiNO$_3$ and NaNO$_2$, reagents purchased from Wako Pure Chemical Industries Ltd., were first heated to about 190°C in a pyrex tube under vacuum to remove water. Subsequently, each specimen was put into a gold container and the container was then sealed. The masses of the specimens and the containers are listed in Table 1.

RESULTS AND DISCUSSION

Test with joule heating

In a conduction calorimeter such as the present one, the actual heat (enthalpy) change must be proportional to the integral of the differential temperature between the calorimetric unit and the isothermal jacket, and the proportionality constant is defined as an apparatus constant. Figure 4 shows this relation for the two cases of the calorimeter operating at 25 and 400°C. The time constants of the decay of the heat flow from the cell to the isothermal jacket were 30 min and 12 min for 25 and 400°C, respectively.

The two solid circles plotted in the figure indicate the experimental points when the duration time of the joule heating was 5 min, which is much longer than the others (30 s). The standard deviation of the data points from the straight line was 1.1%. Good proportionality was thus confirmed for each operating temperature, independent of the duration of the heat change.

The apparatus constant at 400°C is smaller than that at room temperature. That is due to heat flow by radiation from the calorimeter cell to the isothermal jacket, which is larger at higher temperatures.
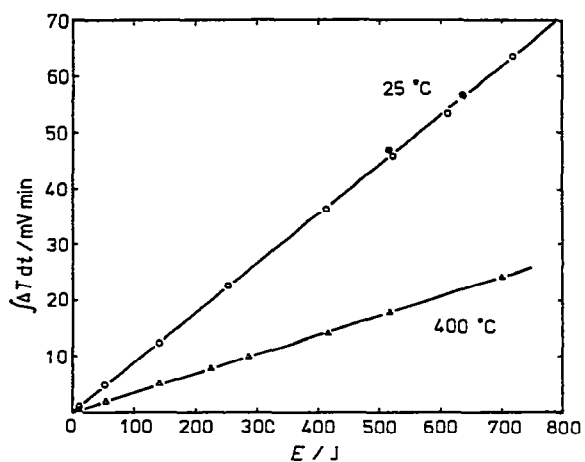
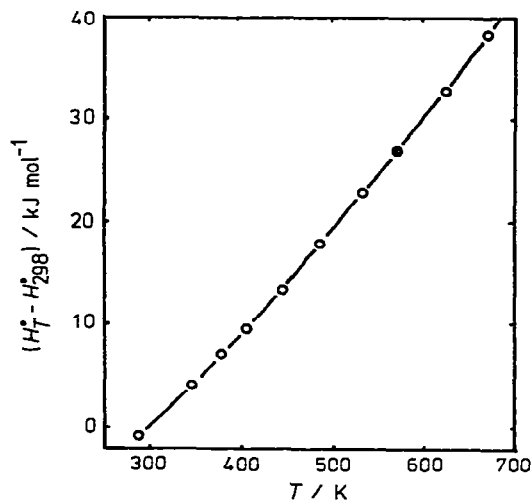Fig. 4. Relation between heat change in the calorimeter cell and integral of the differential temperature.

Fig. 5. Enthalpy change of N.B.S. calorimetric standard sapphire. ○, Present results; ●, reference point (operation temperature of the calorimeter); ——, Ditmars and Douglas [12].

Calibration and test on N.B.S. calorimetric standard sapphire

The calorimeter was operated at 300°C for all the drop measurements and the apparatus constant was determined from the enthalpy changes when the gold containers, with and without the standard sapphire, were dropped from room temperature. The measurements of enthalpy change were performed over the temperature range from 300 to 700 K. The values of enthalpy change determined are plotted in Fig. 5 as open circles, with the solid circle indicating the reference point (the operation temperature).

The heat picked up during the drop was less than 5% of the total enthalpy change of the gold container for all the measurements. The deviations from the literature values [12] (the solid line in the figure) were within 1.5%. The heat capacity was also determined by a differentiation of polynomial equation best fit to the experimental enthalpy values. The result is compared with the literature values [12] in Fig. 6, which shows reasonably good agreement (within 3%) from 400 to 700 K.

Enthalpy of LiNO₃

Figure 7 shows the standard enthalpy change data of $LiNO_3$ together with the literature values by Goodwin and Kalmus [3]. The heat of fusion and the heat capacity of the solid determined from the figure are listed in Table 2 and show good agreement with those of Goodwin and Kalmus. However, the present value of the heat capacity of the liquid is higher than theirs [3]. The reason of this discrepancy is not clear, but it might be due to the impurities in the sample because of its hygroscopic nature. After the completion of this
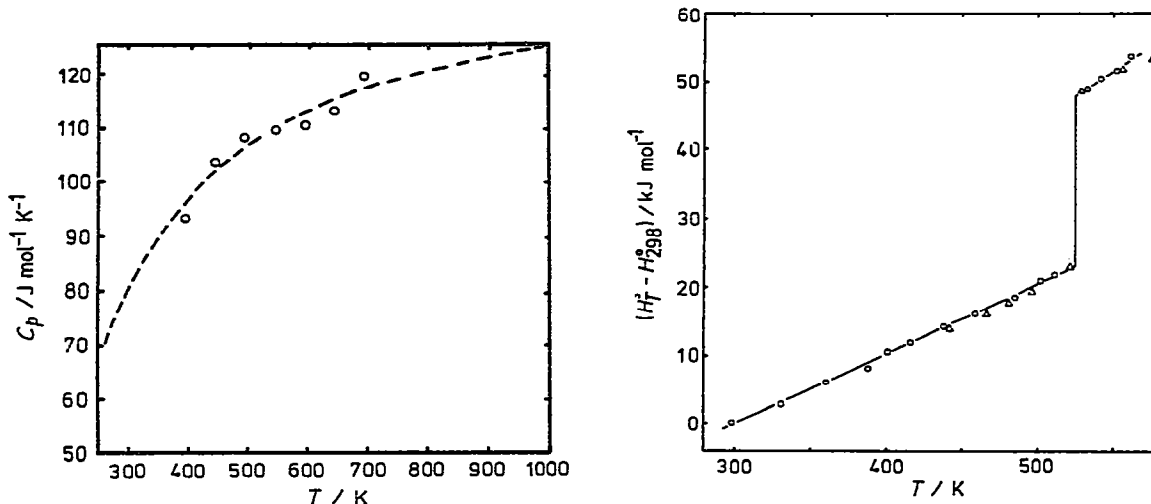
Fig. 6. Heat capacity of N.B.S. calorimetric standard sapphire. O, Present results; — — —, Ditmars and Douglas [12].

Fig. 7. Enthalpy change of LiNO$_3$, O, Present results; △, Goodwin and Kalmus [3].

study, we found the enthalpy measurement by Tye et al. [13], the results of which are also listed in Table 2. Although their heat capacity values are in good agreement with ours, their value for the heat of fusion is much higher than ours and also that of Goodwin and Kalmus.

The entropy of fusion calculated from our results is 11.2 e.u. *, which is very high compared with other nitrates, as can be seen from Table 3. It is well known that lithium nitrate has no thermally detectable transition, whereas other alkali metal nitrates, TlNO$_3$ and AgNO$_3$ have at least one transition. In the table are also listed the entropies of the transitions. It is worth noting that the entropy of fusion of LiNO$_3$ is much higher than the sum of the entropies of transition and fusion of any other nitrate, which is 6—8 e.u.

Some of these transitions are considered to be associated with the ordering of the orientation of the nitrate ion [14,16]. For example, the λ transition of NaNO$_3$, which has a rhombohedral calcite-type [17] structure at room temperature, as well as LiNO$_3$ [18] is due to this ordering effect [19], though the orientation is not completely free in molten NaNO$_3$ as shown by the volume change on fusion [20].

On the other hand, a recent X-ray diffraction analysis by Ohno and Furukawa [21] has shown that there are six near-neighbor cations around the nitrate ion in molten LiNO$_3$ and AgNO$_3$ and that there are three in all other nitrates listed in the table. A pulsed neutron diffraction study by Suzuki and Fukushima [22] has shown that the nitrate ion forms an isosceles triangle in molten LiNO$_3$, AgNO$_3$, and TlNO$_3$, and a regular triangle in molten NaNO$_3$, KNO$_3$, RbNO$_3$, and CsNO$_3$.

---

* 1 e.u. = 4.184 J mole^{-1} K^{-1}.

TABLE 2

Heat of fusion and heat capacity of $LiNO_3$

Ref.	H_f (kJ·mole^{-1})	C_p (solid) * (kJ mole^{-1} K^{-1})	C_p (liquid) * (kJ mole^{-1} K^{-1})
This work	24.6	0.105 (299—525 K)	0.148 (525—552 K)
[3]	25.5	0.111 (442—525 K)	0.112 (525—576 K)
[13]	36.7	0.106 (433 K)	0.150 (553 K)

* The temperature range over which the value of C_p was obtained is shown in parentheses.

Considering these experimental results, the nitrate ion is expected to be in a less freely rotating state in molten $LiNO_3$ and $AgNO_3$. In this connection, the high entropy of fusion of $LiNO_3$ should be attributed mostly to other disorders than to the rotational disorder of the nitrate ion.

Enthalpy of $NaNO_2$

The standard enthalpy change of $NaNO_2$ is shown in Fig. 8. A rather gentle increase around 450 K corresponds to a transition and the jump at a higher temperature indicates fusion. The heat capacity of the liquid was determined to be 0.114 kJ mole^{-1} K^{-1}. The heat capacity of the solid was

TABLE 3

Entropies of transition [14] and fusion [15] for alkali metal, thallium, and silver nitrates (MNO_3)

Cation M	ΔS_t * (e.u.)			ΔS_f * (e.u.)	$\Sigma \Delta S_t + \Delta S_f$ (e.u.)
Li				11.2 (525 K)	11.2
Na	1.88 (549 K)			6.1 (580 K)	8.0
K	2.14 (383 K)	2.07 (397 K)		3.79 (607 K)	8.0
Rb	2.11 (437 K)	1.53 (492 K)	0.42 (564 K)	1.91 (581 K)	6.0
Cs	2.10 (425 K)			4.96 (679 K)	7.1
Tl	0.7 (348 K)	2.18 (416 K)		4.37 (483 K)	7.3
Ag	1.34 (432 K)			6.19 (483 K)	7.5

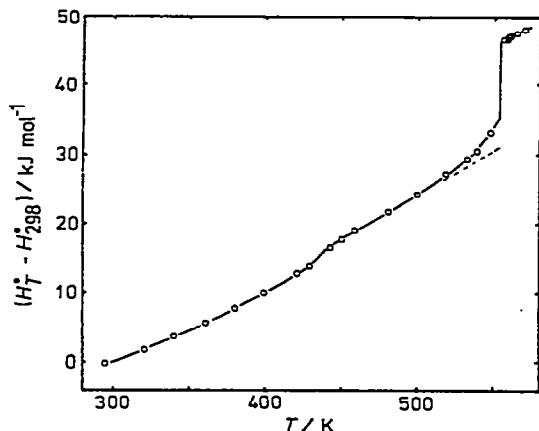* Figures in parentheses indicate the transition and fusion temperatures.

368

Fig. 8. Enthalpy change of $NaNO_2$. O, Present results.

not obtained because of its strong temperature dependence, though it was confirmed that the heat capacity of the solid is higher than that of the liquid. This rather unusual phenomenon is exhibited by some other molten salts [23—25], most of which have transitions. It might be attributed to disordering accompanied by the transitions.

The enthalpy of fusion was determined from the enthapy value of the solid and that of the liquid extrapolated to the melting point, which was determined to be 552 K by DSC. The enthalpy of fusion thus obtained is 15.3 kJ mole^{-1} and the entropy of fusion is 6.6 e.u.

The present results agree very well with those of Cases [4] (0.100 kJ mole^{-1} K^{-1} for the heat capacity of the liquid and 14.9 ± 0.8 kJ mole^{-1} for the enthalpy of fusion) except for the rapid increase of the enthalpy below the melting point. Since no change of the enthalpy value and no weight change were observed after all the measurements, the rapid enthalpy increase is peculiar to the present sample.

The value of the enthalpy of fusion (15.3 kJ mole^{-1}) corresponds to 0.222 kJ g^{-1}, which is higher than that of $NaNO_3$. Therefore $NaNO_2$, as well as $NaNO_3$, could be a good component material for latent-heat storage.

CONCLUSION

A high-temperature calorimeter of the twin type was designed and constructed for the enthalpy measurement of latent-heat storage materials. It was tested with joule heating and the N.B.S. calorimetric standard sapphire. From these tests, the reliability of this calorimeter was confirmed at least over the present temperature range up to 400°C. The enthalpy change of the sapphire was determined with a maximum deviation of ±1.5% from the literature values by Ditmars and Douglas [12] from room temperature to 400°C.

The enthalpy changes of $LiNO_3$ and $NaNO_2$ were measured over the temperature range through the fusion up to 300°C. Although the enthalpy of

fusion of $LiNO_3$ agreed with the value obtained by Goodwin and Kalmus [3], our value for the heat capacity of the liquid was higher than theirs. The high entropy of fusion of $LiNO_3$ should be mainly attributed to disorders other than the rotational disorder of the nitrate ion. The enthalpy of fusion and the heat capacity of $NaNO_2$ determined were in good agreement with the values obtained by Cases [4].

ACKNOWLEDGEMENTS

REFERENCES

1 T.T. Bramlette, R.M. Green, J.J. Bartel, D.K. Ottesen, C.T. Schafer and T.D. Brumlevel, SAND 75-8063, NTIS, U.S. Department of Commerce, 1976.
2 T. Ozawa, M. Kamimoto, R. Sakamoto, Y. Takahashi and K. Kanari, Denshi Gijutsu Sogo Kekyujo Iho, 43 (1979) 289.
3 H.M. Goodwin and H.T. Kalmus, Phys. Rev., 28 (1909) 1.
4 J.C. Cases, Rev. Chim. Mineral., 10 (1973) 577.
5 M. Sakiyama, A. Kimoto and S. Seki, J. Phys. Soc. Jpn., 20 (1965) 2180.
6 I. Hatta and A. Ikushima, Phys. Lett. A, 37 (1971) 207.
7 I. Hatta and A. Ikushima, J. Phys. Chem. Solids, 34 (1973) 57.
8 M. Kamimoto, T. Tanaka, T. Tani and T. Horigome, Sol. Energy, 24 (1980).
9 O.J. Kleppa, J. Phys. Chem., 64 (1960) 1937.
10 C.F. Derrington, A. Navrotsky and M. O'Keeffe, Solid State Commun., 18 (1976) 47.
11 S. Tamura, T. Yokokawa and K. Niwa, J. Chem. Thermodyn., 7 (1975) 633.
12 D.A. Ditmars and T.B. Douglas, J. Res. Natl. Bur. Stand. (U.S.), Sect. A, 75 (1971) 401.
13 R.P. Tye, A.O. Desjarlais and J.G. Bourne, in A. Cezairliyan (Ed.), Proceedings of the Seventh Symposium on Thermophysical Properties, The American Society of Mechanical Engineers, 1977, p. 189.
14 C.N.R. Rao, B. Prakash and M. Natarajan, NSRDS-NBS 53, U.S. Department of Commerce, 1975.
15 J. Lumsden, Thermodynamics of Molten Salt Mixtures, Academic Press, New York, 1966. G.J. Janz, Molten Salts Handbook, Academic Press, New York, 1967.
16 D.M. Newns and L.A.K. Staveley, Chem. Rev., 66 (1966) 267.
17 R.W.G. Wyckoff, Phys. Rev., 16 (1920) 149.
18 H.E. Swansen (Ed.), Natl. Bur. Stand. (U.S.) Circ. 539, 7 (1957) 27.
19 F.C. Kracek, E. Posnjak and S.B. Hendricks, J. Am. Chem. Soc., 53 (1931) 3339.
20 K. Furukawa, Sci. Rep. Res. Inst. Tohoku Univ. Ser. A, 12 (1960) 150; Discuss. Faraday Soc., 32 (1962) 53.
21 H. Ohno and K. Furukawa, J. Chem. Soc., Faraday Trans. I, 74 (1978) 297.
22 K. Suzuki and Y. Fukushima, Z. Naturforsch., 329 (1977) 1438.
23 G.J. Janz, F.J. Kelly and J.L. Pĕrano, J. Chem. Eng. Data, 9 (1964) 133.
24 K.K. Kelley, U.S. Bur. of Mines Bull., (1960) 584.
25 V.A. Sokolov and N.E. Shmidt, Izv. Sekt. Fiz. Khim. Anal., Inst. Obshch. Neorg. Khim., Akad. Nauk SSSR, 26 (1955) 123.